

EMPIRICAL APPROACH TO MOLECULAR INTERACTIONS

V. GUTMANN

Institut für Anorganische Chemie, Technische Hochschule Wien, Getreidemarkt 9, A-1060 Vienna (Austria)

(Received 24 June 1974; in final form 13 November 1974)

CONTENTS

| | |
|--|-----|
| A. Introduction | 207 |
| B. Limitations of the Mulliken theory | 208 |
| C. Inductive effects in adduct formation | 211 |
| (i) General | 211 |
| (ii) Strong adducts | 211 |
| (iii) Weak adducts | 213 |
| (iv) Application of the donicity concept | 214 |
| (v) Coordination involving back donation | 219 |
| D. Inductive effects in adsorption phenomena | 222 |
| E. Inductive effects and reactivity in the crystalline state | 225 |
| (i) Molecular lattices | 225 |
| (ii) Ionic lattices | 226 |
| (iii) Silicate structures | 227 |
| F. Inductive effects in association phenomena | 231 |
| G. Conclusion | 234 |
| H. Acknowledgements | 235 |
| I. References | 235 |

A. INTRODUCTION

A molecular adduct may be defined as the result of the interaction of a neutral Lewis base with a neutral Lewis acid. In such compounds the lattice energies play a minor role, permitting a more straight forward discussion of the coordinating interactions [1].

The term "Molecular Adduct" or "Molecular Complex" embraces a wide variety of diverse substances ranging from the stable coordination compounds such as those formed between ammonia and boron(III)fluoride to weak complexes involving, for example, the interaction between iodine and benzene, the latter being also known as "Charge-transfer Complexes". Although no sharp border line can be drawn between "weak" and "strong" interactions, entirely different approaches are being used for each of these groups of molecular adducts: the normal coordination-chemistry approach is applied to the first group [1], and the Mulliken VB-method to charge-transfer complexes.

es [2-4] which have also been termed "Electron-Donor-Acceptor Complexes" [2]. Hydrogen bond systems and association phenomena in the liquid state are other types of molecular interactions and these have been treated by the electrostatic approach, although its inadequacies are obvious [5] and quantum mechanical considerations are more promising. Other types of molecular interactions are involved in adsorption phenomena and surface chemistry and, as will be shown in this paper, in the crystalline state. Weak complex interactions include also all effects involved in outer-sphere coordination of ions and most ion association phenomena, and these have been discussed elsewhere [7].

Interest in weak complex interactions has accelerated over the past two decades and their importance in biochemistry and biology is now generally recognized [3-6].

The present discussion attempts to give a unified description of all the varieties of molecular interactions irrespective of the stability of the complex species. Emphasis is given to the effects of charge-transfer involved in the formation of molecular compounds, resulting from the intermolecular electron pair donor (EPD)-electron pair acceptor (EPA)-interactions. All changes in charge are transmitted effectively to the other atoms of the molecule [8]. It is hoped that the electronic description may serve to gain a better understanding of the common features of compounds hitherto treated differently.

B. LIMITATIONS OF THE MULLIKEN THEORY

According to Mulliken [2-4, 9-11] the formation of a charge transfer complex is a consequence of electron exchange reactions of second or higher order (resonance energy R_N) and of van der Waals energy contributions W_o . Covalent contributions are considered small and are neglected in this approach. The term "charge-transfer" is used as a label for an electronic transition that is accompanied by a migration of charge from one molecule to another. Hence, the term has no significance if, for example, the ground state of a complex is described by MO-theory; the label, charge-transfer, is, however, useful, when describing a transfer of charge from a donor to an acceptor. The Mulliken treatment only applies to cases in which the donor and acceptor are neutral closed-shell species and are both in symmetrical singlet electronic states [6].

Mulliken considers the enthalpy of charge-transfer complex formation as the sum of the resonance energy between ionic and non-ionic contributions of the molecular ground state R_N and the sum of the van der Waals-energy contributions W_o .

$$\Delta H = R_N + W_o$$

The resonance energy R_N is related to the electron transfer energy $h\nu_{CT}$ and this has been related to the ionization potential of the electron-donating component I_D and to the electron affinity of the electron acceptor E_A . In

simplified form this is represented by the following equation [11].

$$h\nu_{CT} = I_D + E_A + \text{const.}$$

The ionization potential is defined as the energy required to remove the electron completely from the molecule. It is obvious that this reaction is not involved in the course of charge-transfer complex formation. Table 1 reveals that molecules with nearly identical values for the ionization potentials [12], may have vastly different donor-properties, e.g., hexane (10.4 eV) and ethanol (10.5 eV) or carbon disulfide (10.1 eV) and ammonia (10.2 eV).

Thus a relationship between the ionization potential of the donor molecule and the charge-transfer energy or the free enthalpy of complex formation can only exist for a given type of complex compound, i.e., those composed of a given acceptor molecule and of donor molecules with the same functional group [12]. Only in these cases are such relationships actually found, because the effects of different substituents on the donor molecule are reflected in appropriate changes of various molecular properties such as ionization potential, dipole moment, magnetic susceptibility or spectral properties.

For example a relationship exists for molecular adducts of iodine between the ΔH value for adduct formation and the position of the charge-transfer band, $h\nu_{CT}$, as long as donor molecules with the same functional group are considered (Fig. 1). Different lines are obtained in the $\Delta H-h\nu_{CT}$ -plot for π -donor-molecules (curve C), for molecules coordinating through a C—O group (curve B) and for those coordinating through a nitrogen atom (curve A) respectively.

The $\Delta G-h\nu_{CT}$ -plot for iodine complexes (Fig. 2) reveals similar tendencies as shown in the $\Delta H-h\nu_{CT}$ -plot (Fig. 1). There is a fairly good straight line for most of the amines, although triethyl-, tri-*n*-propyl- and tri-*n*-butyl-amine show more positive ΔG values than would be expected from a linear relationship. This may be ascribed to strong entropic changes during the course of complex formation due to steric effects. In many cases, however, the entropic changes appear to remain nearly constant within one homologous series, such as within the series of methylated benzene derivatives.

TABLE 1

Ionization potentials of various donor molecules

| Donor | I_D [eV] | Donor | I_D [eV] |
|------------------|------------|----------------------|------------|
| Trimethylamine | 7.8 | Ammonia | 10.2 |
| Pyridine | 7.9 | Hexane | 10.4 |
| Xylene | 8.3 | Ethanol | 10.5 |
| Benzene | 9.2 | Dichloromethane | 11.3 |
| Diethylether | 9.5 | Chloroform | 11.4 |
| Acetone | 9.7 | Carbon tetrachloride | 11.5 |
| Carbon disulfide | 10.1 | Water | 12.6 |
| Ethyl acetate | 10.1 | | |

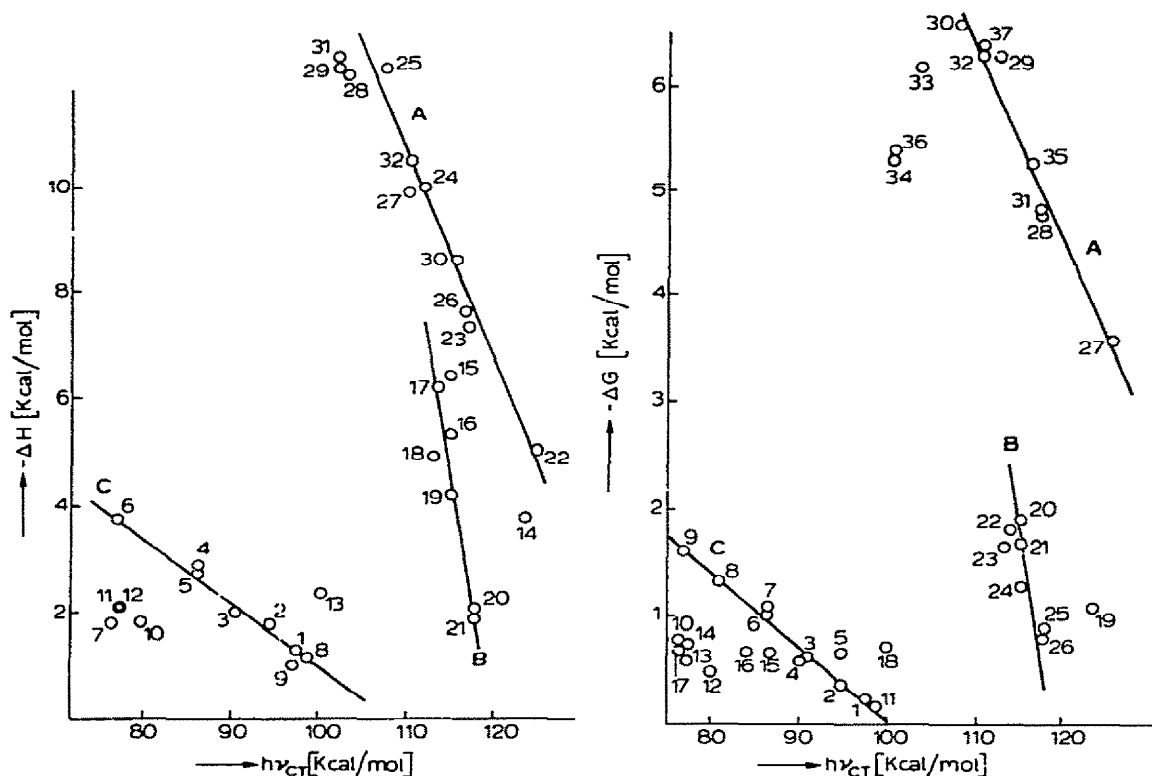


Fig. 1. Relationship between enthalpy of complex formation ΔH and charge-transfer energy $h\nu_{CT}$ for complexes with iodine and different EPD molecules. 1, benzene; 2, toluene; 3, *o*-xylene; 4, mesitylene; 5, durene; 6, hexamethylbenzene; 7, hexaethylbenzene; 8, chlorobenzene; 9, *o*-dichlorobenzene; 10, naphthalene; 11, 1-methylnaphthalene; 12, 2-methylnaphthalene; 13, cyclohexane; 14, propylene oxide; 15, trimethylene oxide; 16, THF; 17, 2-methyl-THF; 18, tetrahydropyran; 19, diethylether; 20, ethanol; 21, methanol; 22, ammonia; 23, methylamine; 24, dimethylamine; 25, trimethylamine; 26, ethylamine; 27, diethylamine; 28, triethylamine; 29, tri-*n*-propylamine; 30, *n*-butylamine; 31, tri-*n*-butylamine; 32, piperidine.

Fig. 2. Relationship between free enthalpy of complex formation ΔG and charge-transfer energy $h\nu_{CT}$ for complexes with iodine and different EPD molecules. 1, benzene; 2, toluene; 3, *o*-xylene; 4, *m*-xylene; 5, *p*-xylene; 6, mesitylene; 7, durene; 8, pentamethylbenzene; 9, hexamethylbenzene; 10, hexaethylbenzene; 11, bromobenzene; 12, naphthalene; 13, 1-methylnaphthalene; 14, 2-methylnaphthalene; 15, styrene; 16, diphenyl; 17, stilbene; 18, cyclohexane; 19, propylene oxide; 20, trimethylene oxide; 21, THF; 22, 2-methyl-THF; 23, tetrahydropyran; 24, diethylether; 25, methanol; 26, ethanol; 27, ammonia; 28, methylamine; 29, dimethylamine; 30, trimethylamine; 31, ethylamine; 32, diethylamine; 33, triethylamine; 34, tri-*n*-propylamine; 35, *n*-butylamine; 36, tri-*n*-butylamine; 37, piperidine.

It may further be questioned, whether a separation of the interaction energy into W_0 and R_N terms is justified, in as much as charge-transfer complexes are closed conjugating systems without "isolated polar groups". It is impossible to explain in this way the differences in behaviour of donor molecules to-

wards iodine depending on the nature of the functional group (Figs. 1 and 2). Amines are much stronger donor molecules than alcohols or ethers although the ionization potentials are similar to those of the latter, as are the charge-transfer energies in the complex compounds.

Analogous considerations may be made concerning the relative acceptor strengths. Charge-transfer energy and electron affinity will be useful only when relative complex stabilities within one homologous series of acceptor molecules towards a certain donor are compared.

C. INDUCTIVE EFFECTS IN ADDUCT FORMATION

i. General

The elucidation of molecular structures of certain adduct molecules of oxocompounds by Lindqvist [1] has considerably widened our views on molecular complexes. Based on structural information he developed a theory for donor-acceptor interaction for oxo-compounds as donor molecules [1], which takes into account both the structural and electronic rearrangements after the formation of the coordinate bond. He formulated the following empirical rule: "The greater the heteropolarity of a bond the lower is its bond order" and "a higher heteropolarity gives a weaker bond, as is manifested in the bond lengths of polar bonds". Consideration is given to the effect of the donor-acceptor bond on adjacent bonds leading to changes in polarity and hence in bond length, as well as to the effects of substituents at a given functional donor group.

The simplest presentation of this is the application of the inductive effects between and within the reacting molecules [7], which may be represented by bent arrows between the atoms. We shall make use of the following rule: The formation of a coordinate bond induces the polarization of the adjacent bonds within the reacting molecules. An inverse relationship exists between the strength of the intermolecular (coordinate) bond and the increase in bond distances of the adjacent intramolecular bonds



ii Strong adducts

Attention to this inverse relationship has been drawn by Prout and Wright [13] from consideration of bond distances in complexes formed from *N*-donors and boron(III)-fluoride. The B—F distances are increased as the *N*→B distances decrease (Table 2) with increasing base strength of the donor (Table 2).

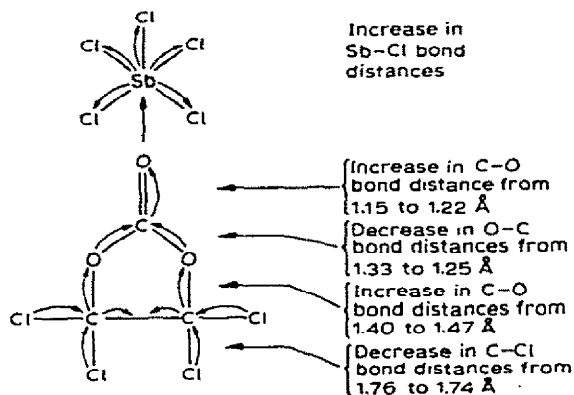
The induced increase in N—H bond length in the ammonia molecule is seen from comparison of the N—H bond distances in ammonia (1.015 Å) and in the ammonium ion (1.031 Å) [14].

TABLE 2

Bond distances in BF_3 and BF_3 adducts in Å [13–15]

| | BF_3 | $\text{CH}_3\text{CN} \rightarrow \text{BF}_3$ | $\text{H}_3\text{N} \rightarrow \text{BF}_3$ | $\text{Me}_3\text{N} \rightarrow \text{BF}_3$ |
|---------------|---------------|--|--|---|
| N→B distance | — | 1.63 | 1.60 | 1.58 |
| B—F distances | 1.30 | 1.33 | 1.38 | 1.39 |

The primary inductive effects may induce subsequent characteristic changes in bond properties throughout the molecules. As a rule, they lead to an increase in σ -bond distance as long as the charge transfer occurs from the more electropositive to the more electronegative atom, and to a decrease in σ -bond distance when the charge transfer is induced into the opposite direction. The features are well demonstrated by considering the adduct formation from tetrachloroethylene carbonate and antimony(V) chloride. Although the ΔH value for this reaction is low [16] the induced changes in bond distances are well pronounced [17].

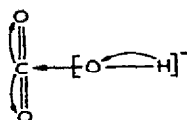


In addition, a decrease in C—C distance from 1.53 to 1.43 Å is induced, suggesting formation of a partial π -bond.

Likewise the formation of the adduct $\text{Cl}_2\text{SeO} \rightarrow \text{SbCl}_5$ through oxygen coordination at the antimony leads to an increase in Sb—Cl bond distances as well as in the Se—O bond distance [18] (primary inductive effect). The increase in polarity of the Se—O bond imposes an increase in positive net charge at the selenium which will attract the electrons more strongly from the chlorine atoms so that secondary effects are induced; in that case the Cl—Se bonds are shortened [1, 18].

Structural data are available for eight SbCl_5 adducts with O donors of different donicity [1, 17, 18]. The greater the donicity of the base, the shorter are the Sb—O distances (stronger coordination) and the greater, although to a smaller extent, the Sb—Cl distances.

In an analogous manner the formation of the hydrogencarbonate ion from carbon dioxide and hydroxide ion may be described. The first step is a strong σ -EPA- n -EPD interaction, as the hydroxide ion functions as a strong base.



Consequently the carbon-oxygen bonds of the CO_2 unit are weakened due to the induced charge transfer leading to an increase in both polarity and bond distance. The $\text{C}=\text{O}$ distance is 1.159 Å in the carbon dioxide molecule and in the hydrogencarbonate ion two $\text{C}=\text{O}$ bond lengths are 1.263 Å while the third with the hydrogen atom attached shows a $\text{C}-\text{O}$ bond distance of 1.346 Å [19]. A partial charge transfer from the hydrogen atom to the oxygen atom is also induced and this leads to the development of weakly acidic properties at the hydrogen atom. Table 3 shows further examples for the increase in $\text{M}-\text{X}$ distances due to coordination.

iii Weak adducts

For weak molecular complexes by far the largest contribution to crystal structures has come from Hassel and his co-workers [20]. In the majority of the structures the donor atoms are nitrogen, oxygen, sulfur or selenium atoms and the acceptor molecules are halogen, interhalogen or halogen-rich

TABLE 3

Bond distances $\text{M}-\text{X}$ in EPA molecules and in their complex compounds [1, 14]

| EPA molecule | $\text{M}-\text{X}$ (Å) | Complex ion | $\text{M}-\text{X}$ (Å) |
|-----------------|-------------------------|------------------------|-------------------------|
| CdCl_2 | 2.235 | $[\text{CdCl}_6]^{4-}$ | 2.53 |
| SiF_4 | 1.54 | $[\text{SiF}_6]^{2-}$ | 1.71 |
| TiCl_4 | 2.18–2.21 | $[\text{TiCl}_6]^{2-}$ | 2.35 |
| ZrCl_4 | 2.33 | $[\text{ZrCl}_6]^{2-}$ | 2.45 |
| GeCl_4 | 2.08–2.10 | $[\text{GeCl}_6]^{2-}$ | 2.35 |
| GeF_4 | 1.67 | $[\text{GeF}_6]^{2-}$ | 1.77 |
| SnBr_4 | 2.44 | $[\text{SnBr}_6]^{2-}$ | 2.59–2.64 |
| SnCl_4 | 2.30–2.33 | $[\text{SnCl}_6]^{2-}$ | 2.41–2.45 |
| SnI_4 | 2.64 | $[\text{SnI}_6]^{2-}$ | 2.85 |
| PbCl_4 | 2.43 | $[\text{PbCl}_6]^{2-}$ | 2.48–2.50 |
| PF_5 | 1.54–1.57 | $[\text{PF}_6]^-$ | 1.73 |
| SbCl_5 | 2.31 | $[\text{SbCl}_6]^-$ | 2.47 |
| SO_2 | 1.43 | $[\text{SO}_3]^{2-}$ | 1.50 |
| SeO_2 | 1.61 | $[\text{SeO}_3]^{2-}$ | 1.74 |
| ICl | 2.30 | $[\text{ICl}_2]^-$ | 2.36 |
| I_2 | 2.66 | $[\text{I}_3]^-$ | 2.83 |

TABLE 4

Halogen—halogen bond length in halogen molecular complexes [24]

| Compound | Halogen—halogen bond length | |
|---|-----------------------------|------------|
| | Free | In complex |
| 1,4-Dioxane-Br ₂ (chain structure) | 2.28 | 2.31 |
| 1,4-Dioxane-Cl ₂ (chain structure) | 1.99 | 2.02 |
| 1,4-Dithiane-I ₂ | 2.67 | 2.79 |
| 1,4-Diselenane-I ₂ | 2.67 | 2.87 |
| Hexamethylenetetramine-2 Br ₂ | 2.28 | 2.43 |
| Trimethylamine-I ₂ | 2.67 | 2.83 |
| Trimethylamine-ICl | 2.32 | 2.52 |
| pyridine-ICl | 2.32 | 2.51 |
| γ -picoline-I ₂ | 2.67 | 2.83 |

haloalkanes [20]. The general features are in accordance with those observed for strong interactions: in the acceptor unit the bond adjacent to the coordinate bond is weakened as seen from the increase in bond length due to coordination (Table 4).

The structures of pyridine—iodine or ether—iodine are in agreement with the principles known for polar acceptor molecules and in contrast to the prediction from the overlap and orientation principle [21]. In trimethylamine-iodine [22] and trimethylamine-iodine monochloride [23] the $N \rightarrow I-I$ and $N \rightarrow I-Cl$ systems are linear and the $N-I$ distances are 2.27 and 2.30 Å respectively. This is 1.4 Å less than the sum of the van der Waals radii and only 0.3 Å greater than the sum of covalent radii. The $I-I$ distance in the complex is 0.17 Å longer than in free iodine and the $I-Cl$ distance in the complex 0.22 Å longer than in the free acceptor molecule.

The increase in halogen—halogen bond distance by complexation is least pronounced when donor and acceptor molecules contain two suitable coordinating sites: the 1,4-dioxane bromine complex [25] and the 1,4-dioxane chlorine complex [26] form two-dimensional structures of endless chains of alternating halogen molecules and 1,4-dioxane molecules. In such compounds the charge transfer effects are weak or non-apparent. For example, in the benzene—bromine complex the benzene and halogen molecules form donor—acceptor stacks with the halogen—halogen bond co-incident with the perpendicular through the centroid of the benzene ring plane and indeed the halogen—halogen distance is no different from that found in the free halogen molecule [27].

iv Application of the donicity concept

The strength of a coordinate bond will depend on the donicity of the

EPD and on the acceptivity of the EPA unit [7]. Since no values are available for the latter, only the relative effect of the donicity can be followed towards a given acceptor component.

Changes in properties of the bonds adjacent to the coordinate link are of great interest. All structural information shows that the bonds within the functional groups of both donor and acceptor molecules become polarized by the formation of the coordinate bond, in agreement with Lindqvist's theory of the donor-acceptor bond [1].

Niendorf and Paetzold [28] have shown that force constants of the bond in the coordinating group of the donor component are related to the thermodynamic stabilities of the molecular adduct. Since changes in bond properties cannot be compared for bonds between different atoms, it follows that such relationships are confined to donor molecules with the same functional group. Hence the decrease in force constant of the P=O group in phosphoryl compounds corresponds to the increase in complex stability related to the donor properties of the phosphoryl group. The same applies to the changes in force constants of the C=O group in carbonyl compounds, but one cannot expect to find such relationships for different functional groups (Fig. 3).

We may therefore turn our attention to changing bond properties by coordination within the acceptor component in the molecular adduct. Burger and Fluck [29] found a nearly linear relationship between the donicity and the electron binding energy of SbCl_5 in quick frozen solutions of excess EPD with different functional groups in dichloroethane. As the electron binding energy at the antimony is increased by increasing donicity (DN) (Fig. 4), it follows that an appropriate decrease in bond strength of the antimony-chlorine bonds is induced by coordination.

Evidence is also available for weak molecular adducts to extend the rela-

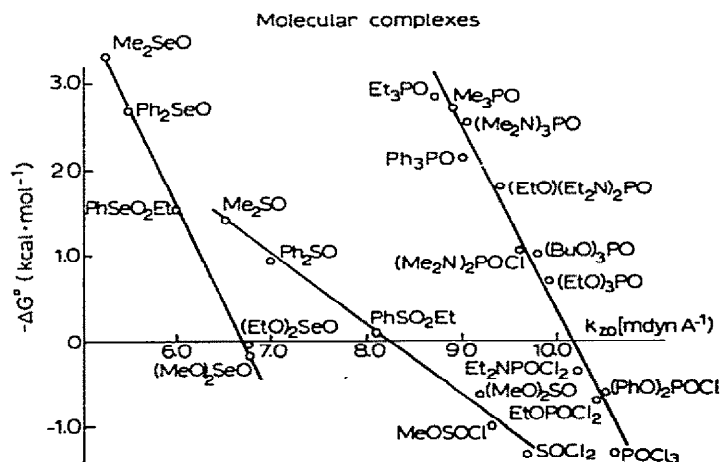


Fig. 3. Relationship between ΔG^0 for the complex equilibria $\text{EPD} + \text{I}_2 \rightleftharpoons \text{EPD} \cdot \text{I}_2$ and the valence force constant of the coordinate group ZO of EPD.

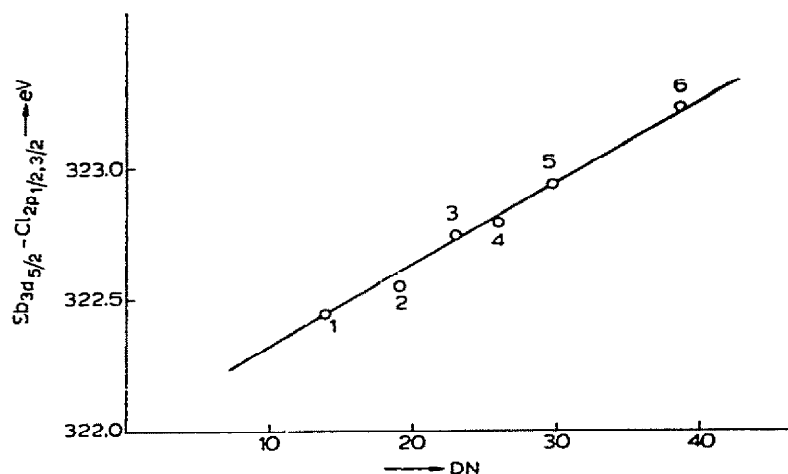


Fig. 4. The electron-binding energies of 3 $d_{5/2}$ orbitals of antimony measured in quick-frozen solutions of SbCl_5 with different EPD molecules in $\text{C}_2\text{H}_4\text{Cl}_2$ vs. the donicity of the EPD molecules. 1, nitrobenzene; 2, acetonitrile; 3, acetone; 4, ethyl acetate; 5, DMF; 6, HMPA.

tionship between donicity and induced bond polarization. Trifluoroiodomethane contains a polarized iodine—carbon bond with the partial positive charge residing at the iodine atom (due to the strong electron attracting properties of the CF_3 group). While with very weak Lewis bases no substantial interactions occur, the plot of ΔH vs. the donicity of the base shows the ΔH values rising with increasing donicity of the latter (Fig. 5), the ΔH values being below 6 kcal mol^{-1} [30].

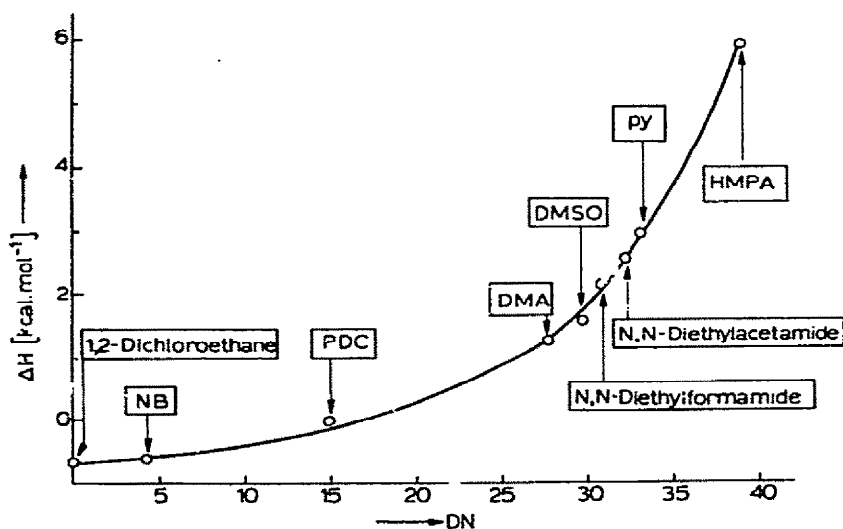


Fig. 5. Enthalpy of charge transfer complexation ΔH between CF_3I and various EPD solvents vs. solvent donicity (NB = nitrobenzene).

The induced polarization of the carbon—fluorine bonds can be seen from ^{19}F NMR data [30], as an increase in electron density at the fluorine atoms attached to the carbon atom produces a shift towards higher field [31].

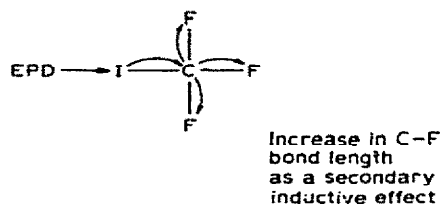


Figure 6 shows the result of titrations of trifluoroiodomethane with different EPD molecules in solutions of nitromethane: the ^{19}F NMR chemical shifts are increased by increase in donicity and the final values reached at decreasing EPD content with increasing donicity [12, 30].

Figure 7 shows that a linear correlation exists between ^{19}F chemical shift and donicity of the EPD. No relationship is found between chemical shift and dipole moments, ionization potentials, polarizabilities or dielectric constants of the EPD. Thus the extent of induced polarizations of the bonds in the EPA units is governed by the EPD functions exerted by the Lewis base. It is important to note that unlike all other relationships for molecular adducts the δ -DN-relation is not confined to complexes with the same functional group, as the relationship holds for different donor groups such as the nitro-group, nitrile-group, C=O, S=O, P=O groups, as well as for ethers and nitrogen-donating bases [12, 30, 32]. This result is significant in that it shows that the functional approach [32] and the donicity concept can be applied

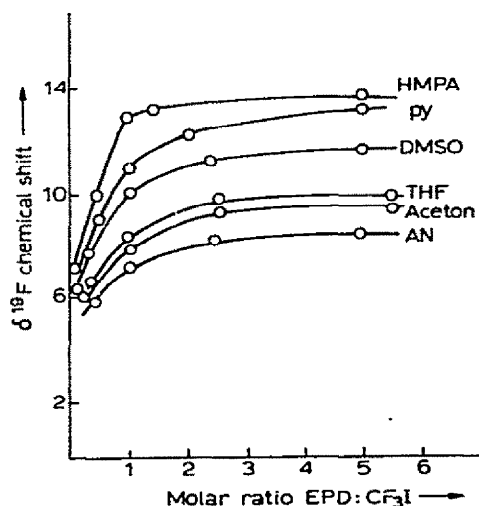


Fig. 6. ^{19}F chemical shifts in CF_3I on addition of neutral EPD at 25°C (in p.p.m. CF_3I as external standard).

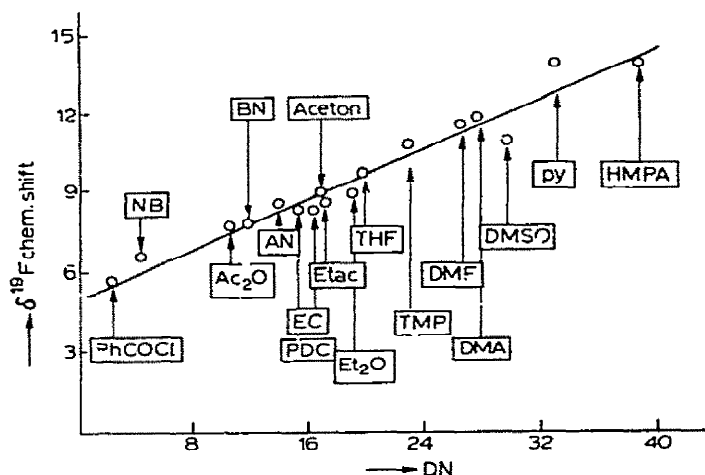


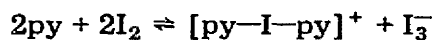
Fig. 7. ^{19}F NMR chemical shifts of CF_3I in EPD solvents at infinite dilution vs. donicity of EPD.

to weak interactions, which have been considered as being mainly due to van der Waal's forces or intermolecular forces in the sense of Mulliken's theory.

It may be concluded that the phenomenological property of the donicity is related not only to the strength of the coordinate bond with a given EPA but also to the extent of the induced changes in bond properties within the complex.

As long as there is a relationship between DN and pK_b value [33] a nearly straight line is also found in the $pK_b - \log K$ plot (K = formation constant of the respective complex) and this is shown in Fig. 8 for EPD- I_2 complexes. In these the halogen-halogen stretching frequencies vary inversely with the strength of the complex: an increase in coordinate bond strength is accompanied by a progressive weakening of the interhalogen bond [34].

A very strong donor may heterolyse this bond, as is indicated by interaction of iodine with excess pyridine, to give cations with equivalent N—I- distances of 2.16 Å [13, 35].



Most molecular adducts are weak because the bonds in the acceptor molecule would be heterolyzed by stronger coordinating interactions [13, 35]. It may therefore be concluded that a molecular adduct is formed by EPD-EPA interactions as long as the adjacent bonds are polarized to the limited extent that heterolytic bond cleavage does not take place. In other words, a molecular adduct may be characterized as the result of well-balanced EPD-EPA interactions which are not sufficient for heterolysis of any of the adjacent bonds. Indeed, there is also a close relationship between donicity of the EPD and the ionization constant [35].

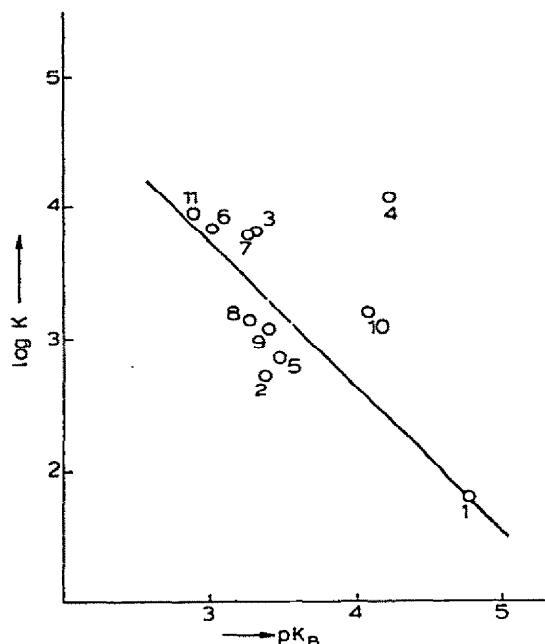
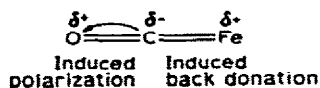


Fig. 8. Relationship between Formation Constant K of complexes between iodine and various amines in *n*-heptane and the basicity constants K_b of the amines in water. 1, ammonia; 2, methylamine; 3, dimethylamine; 4, trimethylamine; 5, ethylamine; 6, diethylamine; 7, triethylamine; 8, tri-*n*-propylamine; 9, *n*-butylamine; 10, tri-*n*-butylamine; 11, piperidine.

v Coordination involving back donation

The electronic features in neutral complexes, formed from neutral species, are essentially the same when back-donation is involved. In metal-carbonyl complexes the C—O bond distances are greater than in the free carbon monoxide molecule in which the C≡O distance is 1.128 Å [36] (Table 5).

The weakening of the C≡O bonds by complexation may be represented by the withdrawal of electrons from the C≡O ligand towards the metal as a result σ -dative bond formation. In order to give a full account of the actual bonding, back-donation must be taken into consideration. This effect leads to charge transfer to a greater extent than that involved in σ -bond formation and the final electronic state of the bond may be represented as follows.



This representation is in accordance with the relationship between C—O and C—Fe distances in different iron(0)-carbonyl compounds: The stronger the coordination, e.g. the stronger the Fe—C bond, the weaker is the C—O bond (Fig. 9 and Table 6).

TABLE 5

C—O bond distances in carbonyl compounds [36, 37]

| Complex | C—O bond distance (Å) |
|---------------------------------------|-----------------------|
| H ₃ B—CO | 1.15 ± 0.03 |
| Fe(NO) ₂ (CO) ₂ | 1.14 ± 0.03 |
| Co(NO)(CO) ₃ | 1.14 ± 0.03 |
| Co(CO) ₄ H | 1.16 ± 0.05 |
| Fe(CO) ₄ H ₂ | 1.15 ± 0.05 |
| Ni(CO) ₄ | 1.15 ± 0.02 |
| Fe(CO) ₅ | 1.145 ± 0.003 |
| Mo(CO) ₆ | 1.15 ± 0.05 |
| Cr(CO) ₆ | 1.16 ± 0.05 |

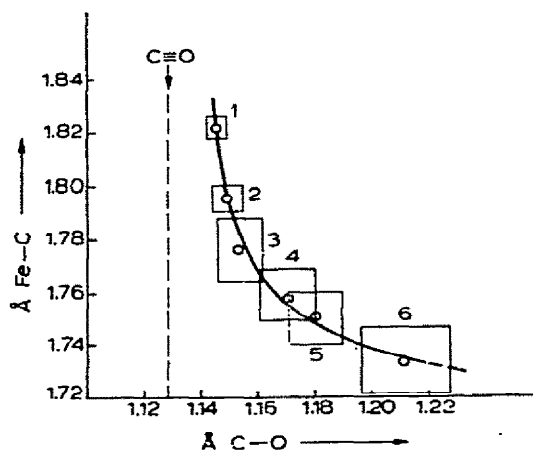


Fig. 3. Relationship between Fe—C and C—O bond distances in different iron carbonyls. 1, Fe(CO)₅; 2, Mn₂Fe(CO)₁₄; 3, Fe₂(CO)₈(C₆H₅C₂H)₃; 4, Fe₂(CO)₆C₆H₅C₂C₆H₅; 5, Fe₂(CO)₆X*; 6, Fe₂(CO)₆(C₂H₂)₃.

* X = [CH₃—C₆H₄—SO₂—N = C(OCH₃)—CH = CH—C(OCH₃)₂].

TABLE 6

Mean values for Fe—C and C—O distances in different iron(0)-carbonyls

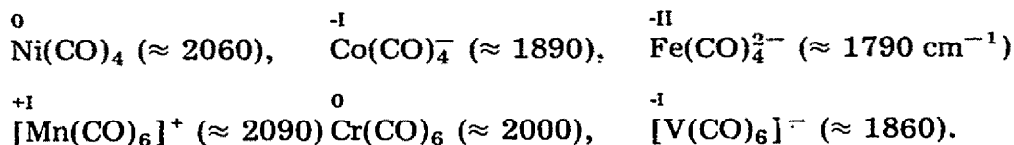
| Compound | Fe—C [Å] | C—O [Å] | Ref. |
|--|---------------|---------------|------|
| Fe(CO) ₅ | 1.822 ± 0.003 | 1.145 ± 0.002 | 38 |
| Mn ₂ Fe(CO) ₁₄ | 1.795 ± 0.005 | 1.150 ± 0.005 | 39 |
| Fe ₂ (CO) ₈ (C ₆ H ₅ C ₂ H) ₃ | 1.775 ± 0.012 | 1.153 ± 0.008 | 40 |
| Fe ₂ (CO) ₆ C ₆ H ₅ C ₂ C ₆ H ₅ | 1.758 ± 0.010 | 1.171 ± 0.010 | 41 |
| Fe ₂ (CO) ₆ X* | 1.75 ± 0.01 | 1.18 ± 0.01 | 42 |
| Fe ₂ (CO) ₆ (C ₂ H ₂) ₃ | 1.733 ± 0.013 | 1.212 ± 0.016 | 43 |

* X = [CH₃—C₆H₄—SO₂—N=C(OCH₃)—CH=CH—C(OCH₃)₂]

The stabilization of the lower oxidation state of the metal is intimately connected with the utilization of the d electrons in π bond formation. Indeed, the changes in oxidizing properties at the metal due to complex formation reveal an increase in oxidizing properties (higher fractional positive charge) [44].

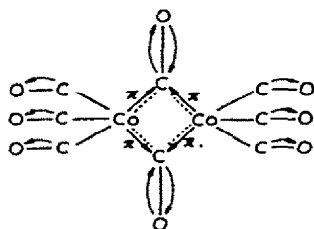
This conclusion is also in agreement with IR data. In carbonyl complexes the carbonyl-stretching frequencies are lower than in free carbon monoxide, where the carbonyl stretching frequency is found at 2168 cm^{-1} . This corresponds to a lower bond order of complexed CO, which is particularly lowered when strongly electron donating ligands, such as phosphines or amines are coordinated at the metallic coordination center. Ligands of high donicity increase the availability of d electrons of the metal for back donation and this is reflected in a decrease in metal-carbon bond distance as well as in the induced lowering of the carbon-oxygen bond order, which may even approach a value nearly corresponding to a C=O bond present in ketonic carbonyls.

Back donation is also enhanced by lowering the oxidation number of the metal and this is reflected in progressive lowering of the C—O stretching frequencies in isoelectronic and isostructural species [45]



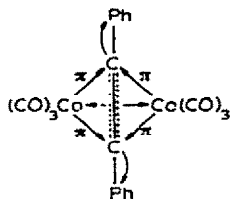
It should also be pointed out that the CO valence frequencies (and the NO frequencies in NO compounds) also depend on the electronic effects of the solvents [45].

The electronic effect induced in a C—O bond is particularly great when the CO group acts as a bridging ligand as can be seen in the compound [46].



In this compound the C—O bond lengths are 1.16 for the terminal and 1.20 Å for the bridging ligands.

The same trend is found for the variation of $\text{C}\equiv\text{C}$ bond lengths upon coordination. In the compound



the C—C bond length is increased from 1.19 Å in free diphenylacetylene to 1.46 Å in the compound $\text{Co}_2(\text{CO})_6\text{Ph}_2\text{C}_2$ [47]. As a secondary electronic effect the C—C_{Ph}-bond distance is increased from 1.40 to 1.42 Å. The C—O bonds are considerably longer than in $\text{Co}_2(\text{CO})_8$ namely 1.23 Å. According to the considerations of Fig. 9 one would expect a shorter Co—C distance than in $\text{Co}_2(\text{CO})_8$ and this is actually found (Co—C 1.75 Å as compared to 1.80 Å in $\text{Co}_2(\text{CO})_8$).

We have seen that induced electron changes along a σ -bond may result in either an increase or a decrease in bond length. The actual effect is largely influenced by the direction of the charge transfer: increase in bond length usually results through an electron shift from the more electropositive to the more electronegative atom and decrease in bond length from the electron shift in the opposite direction. The situation appears to be less differentiated for π -bonds, the bond order of which is decreased by coordination in any case.

D. INDUCTIVE EFFECTS IN ADSORPTION PHENOMENA

All interactions that occur at interfaces are, in principle, of the charge transfer type. Two distinct types of adsorption, physical and chemical adsorption [48, 49], are usually differentiated.

Physical adsorption, or physisorption, is regarded as due to forces of the van der Waals type. The bonds between adsorbent and adsorbate are weak, usually of the order of 5 kcal mol⁻¹ or less. This is of the same order of magnitude as the heat of vaporization of the adsorbate, lending credence to the concept of weak physical bonding [48].

Chemical adsorption, or chemisorption, is characterized by high heats of adsorption, usually of the order of 15–20 kcal mol⁻¹, and hence by strong chemical interaction with the unsaturated surface.

Infrared investigations revealed that characteristic changes are observed in the adsorbate which are due to charge transfer interactions for both types of adsorption differing only in magnitude. For this reason any choice of borderline between these two kinds of interactions is rather arbitrary. An exact differentiation between physisorption and chemisorption is therefore unprofitable and will not be pursued in this review article.

The present situation is very well characterised by Yates's statement [50]: "The outcome of the joint efforts between chemists and physicists, experimentalists and theorists will be a new level of understanding of the electronic nature on solid surfaces and adsorbed layers, a level comparable to that of understanding in structural inorganic and organic chemistry".

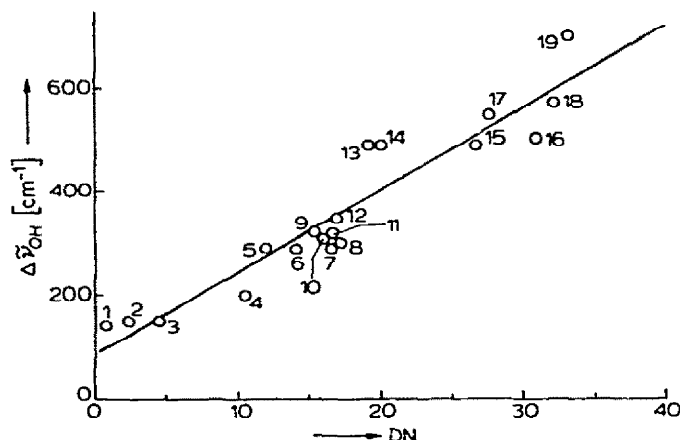
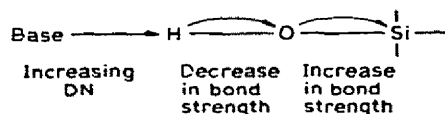


Fig. 10. Relationship between $\Delta\nu_{\text{OH}}$ on aerosile and the donicity of adsorbed solvents. 1, acetyl chloride; 2, benzoyl chloride; 3, nitrobenzene; 4, acetic anhydride; 5, benzonitrile; 6, acetonitrile; 7, methyl acetate; 8, ethyl acetate; 9, iso-butyronitrile; 10, propionitrile; 11, *n*-butyronitrile; 12, acetone; 13, diethylether; 14, tetrahydrofuran; 15, dimethylformamide; 16, diethylformamide; 17, dimethylacetamide; 18, diethylacetamide; 19, pyridine.

A large variety of problems related to the nature of adsorption processes have been studied by infrared spectroscopy and, in principle at least, it is possible to determine from spectral data in detail the chemical functionality of a surface, the induced structure of an adsorbed species and their interactions and interrelationships [51].

The surfaces that have been most studied by the infrared technique are those of silica materials. Even after careful dehydration hydrogen atoms remain on the surface and these are referred to as "free hydroxyl groups" or "isolated silanol groups" [52]. The terminal hydrogen atoms are acidic and readily adsorb basic materials. Even benzene is adsorbed due to the interaction between a surface hydroxyl group and the π electron system of the aromatic molecule. The spectrum of the adsorbed benzene is little but distinctively different from that of the liquid [53]. Nitrobenzene behaves in an analogous manner, while aromatic amides and phenols appear to interact by means of their basic nitrogen and oxygen atoms, respectively [48], towards the acidic hydrogen atoms of the silica surface. Noller and Horill [54] followed the changes in OH-valence frequency by adsorption of a variety of Lewis bases on aerosile. The $\Delta\nu_{\text{OH}}$ values were found to show a linear relationship to the donicity of the adsorbate and to be independent of the nature of coordinating group (Fig. 10). No relationship was found with the ionization



potential of the base. The fact that no correlation was found with the heats of adsorption suggests that adsorption does not occur exclusively at the OH groups.

The adsorption of acetylenes and derivatives on alumina and silica were also explained in terms of acid-base concepts. IR spectra suggest that chemisorbed acetylene and methylacetylene is held normal to the surface since the acidic protons of the adsorbate interact with the basic oxygen sites at the surface. On the other hand the non-acidic dimethylacetylene is held parallel to the surface, as the π electrons of the $C\equiv C$ bond behave as a base and interact with the acid sites of the alumina surface [55].

Adsorption of triphenylchloromethane on barium sulfate showed that the C-Cl bond was strongly polarized and the spectrum of the adsorbate was identical to that of the triphenylcarbonium ion as observed in sulfuric acid solution [56];



The reverse situation was found when symmetrical trinitrobenzene was adsorbed on magnesium oxide, where it was red in contrast to adsorption on CaF_2 . The spectrum of the adsorbed species was very similar to that obtained in alkaline ethanol solution and this led to the conclusion that the oxide ions of the magnesium oxide surface functioned as basic groups for the chemisorption of trinitrobenzene.

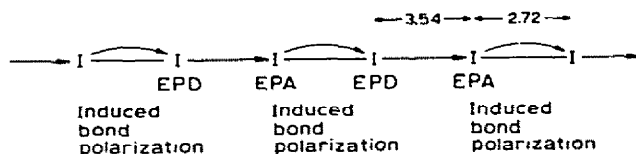
The most extensive and productive application of the IR technique has been in studies of chemisorption on supported metal samples. After the more conventional catalytic research has concentrated on actual catalysts, it is very important that investigations on atomically clean single crystal surfaces have recently been initiated. Yates and King [57] have shown that the so-called α -CO state of CO adsorbed on a clean tungsten surface is similar to "carbonyl"-type CO ligands as found in $W(CO)_6$, in which the C-O bonds are considerably polarized due to back donation (see section C, v). As the CO coverage increases, a slight strengthening of the C-O bond is found. This has been explained by the back-donation mode [57]. The availability of tungsten d electrons for back donation would be expected to decrease with increasing CO coverage both from primary tungsten atoms (those involved directly in the linear $W=C=O$ species) and from neighbouring atoms, which also appear to contribute to π bonding at least at interstitial sites. This is in agreement with the finding that the photoelectron C (1 s) and O (1 s) binding energies for the adsorbed species are all lower than for the gaseous molecules and that there is a systematic decrease in photoelectron binding energy as the adsorption is increased [58].

All the features are in agreement with the postulate of the inverse relationship between intermolecular and intramolecular bond strengths.

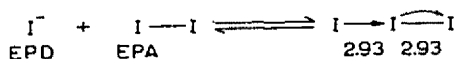
E. INDUCTIVE EFFECTS AND REACTIVITY IN THE CRYSTALLINE STATE

i Molecular lattices

The formation of a molecular lattice from the gaseous molecules may be considered due to intermolecular coordinating interactions. These are expected to induce characteristic changes in intramolecular bond lengths and bond properties. Indeed, the structural features in molecular lattices are phenomenologically analogous to those found in molecular adducts. While the iodine—iodine distance in gaseous iodine is 2.676 Å [59], the intramolecular iodine—iodine distance in the crystalline state is slightly greater, 2.715 Å [60]. From a study of quadrupole coupling [61] it has been concluded that in crystalline iodine the 3.54 Å intermolecular contacts contain about 9% of covalent bonding. Any such covalent interactions should be of the EPD—EPA type which induce an increase in intramolecular bond distance; this may be schematically represented as follows.



This representation describes the formation of the molecular lattice from the gaseous molecules and expresses the different functionalities of iodine atoms connected by the same bond; it is analogous to that for triiodide ion complex formation from iodide ion and molecular iodine. Since iodide ion acts as a considerably stronger EPD than iodine, the polarization of the I—I bond in the iodine molecule which acts now as EPA, is considerably greater, the I—I distances in the triiodide being equal (2.93 Å) [62].



The differences in EPD properties of iodine and iodide ion are also evident from their different solubilities and enthalpies of solvation in water.

The induced charge transfer effects are, as may be expected, slightly more pronounced in iodine bromide. The I—Br distance is 2.52 in solid IBr and 2.47 Å in the gaseous state [63]. The longer intramolecular I—Br distances in the solid state have been regarded as due to the charge transfer between the molecules in the crystal.

We may postulate that there is an inverse relationship between the intermolecular and the intramolecular bond distances within a crystal lattice. The limiting cases are (a) the intermolecular interactions are too weak in order to give measurable intramolecular effects, (b) the intermolecular interactions are so strong, that inter- and intramolecular bond distances and properties are equal and hence undistinguishable.

ii Ionic lattices

Although it may appear strange to treat an ionic crystal like a molecular adduct, one may attempt to apply this approach to the formation of an ionic crystal from the gaseous molecules. The charge transfer incurred in the formation of an alkali halide crystal may be considered a result of coordinating interactions between the gaseous alkali metal halide molecules. Alkali metal ions are known to function as stronger Lewis acids than molecular iodine, and halide ions as stronger Lewis bases than iodine. Hence the induced polarizing effects should be appreciably higher than in the molecular lattice of iodine. The metal-halide distances are significantly greater in the crystalline lattice, than in the gaseous molecules (Table 7).

The relative differences Δd in bond length of the diatomic alkali halide molecules, and of the respective crystal lattice show a decrease from Li^+ to Rb^+ for a given anion as well as from Cl^- to I^- for a given cation. According to the electrostatic approach this is explained by the increasing polarizing power of the alkali metal ions from Rb^+ to Li^+ and the increase in polarizabilities from Cl^- to I^- . Increasing covalent character of the bond is accompanied by decreasing bond distance, as may be seen from the comparison of Ag-X bond distances calculated from ionic radii and actually found.

The electronic description of inductive cooperative charge transfer effects

TABLE 7

Alkali metal-halogen bond distances in alkali halide diatomic molecules and within the crystal lattice [36]

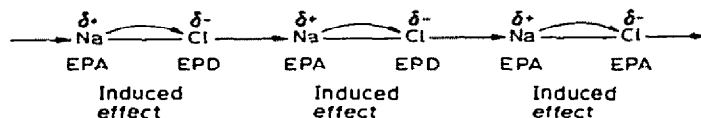
| Halide | M-X distances (Å) | | Δd (Relative increase in M-X distance) |
|--------|-------------------|---------|--|
| | Vapor | Crystal | |
| LiBr | 2.1704 | 2.747 | 26.5% |
| NaBr | 2.5020 | 2.981 | 19.1% |
| KBr | 2.8207 | 3.293 | 16.8% |
| RbBr | 2.9448 | 3.434 | 13.8% |
| LiI | 2.3919 | 3.025 | 26.5% |
| NaI | 2.7115 | 3.231 | 19.1% |
| KI | 3.0478 | 3.526 | 15.8% |
| RbI | 3.1769 | 3.663 | 15.1% |
| KCl | 2.6666 | 3.147 | 18.0% |
| KBr | 2.8207 | 3.293 | 16.8% |
| KI | 3.0478 | 3.526 | 15.8% |
| RbCl | 2.7868 | 3.285 | 17.9% |
| RbBr | 2.9448 | 3.434 | 16.8% |
| RbI | 3.1769 | 3.663 | 15.1% |

TABLE 8

Ag—X bond distances

| AgX | r_X | $r_{Ag} + r_X$ (calc.) | Ag—X (found) | Δ |
|------|-------|---------------------------|-----------------|----------|
| AgF | 1.33 | 2.46 | 2.46 | 0.0 |
| AgCl | 1.81 | 2.94 | 2.77 | —0.17 |
| AgBr | 1.96 | 3.09 | 2.88 | —0.21 |
| AgI | 2.20 | 3.33 | 2.80 | —0.53 |

involved in changing from the gaseous to the crystalline state provide an alternative explanation. The Na—Cl bonds are polarized by the EPD actions of the chloride ions and the EPA actions by the alkali metal cations as shown for one dimension only.



For a given cation the effect of the relative EPD functions of the halogens increases from iodide to chloride.

The interatomic distances of alkali halide vapors obtained from early electron diffraction studies were consistently higher than those now derived from microwave spectroscopy and this is interpreted as due to the presence of polymeric molecules in the vapor. Indeed mass spectrometric analysis of the ions shows the presence of dimers, trimers and in some cases tetramers [64], particularly for lithium halides.

The quantitative aspects of the electrostatic treatment for hard—hard ionic interactions are superior to the approach from the covalent point of view. On the other hand, it should be of interest to note that all structural changes may be described by means of the functional approach, at least in a qualitative way, in that the effects within a crystal lattice are considered as emerging from coordinate interactions which lead to specific changes in covalent bond properties as a result of charge transfer effects between the ions.

iii Silicate structures

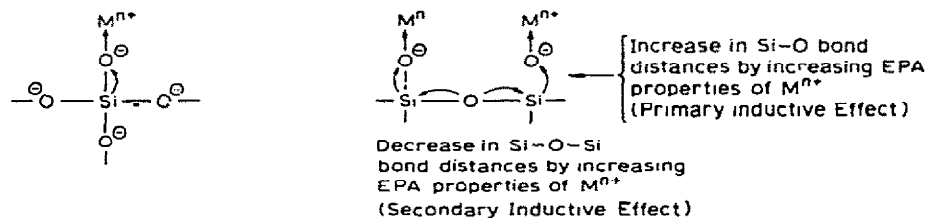
The application of the postulate of the inverse relationship between intermolecular and intramolecular distances to silicate structures is less straight forward, since the properties of the “free” molecules or isolated groups are not known. The variations in Si—O bond lengths in different silicates are correlated with Pauling bond strengths s [65], which is defined as the valence Z of a cation divided by its coordination v [65, 67]. According to the Pauling electrostatic valence principle the sums $p = \sum s$ of mean bond strengths around

the cations and anions are approximately equal to their valence. This concept is derived from an ionic model of chemical bonding, but it can be applied to situations where the bonding is primarily covalent; it has been tested frequently by mineralogists.

The Pauling bond strength is used as an approximate measure of the potential of the cation on the anion site in an undistorted coordination site and hence in silicates it is related to the bond length of the intramolecular Si—O bonds within the anionic groups [66]. It may be postulated that in the non-existing ideally isolated SiO_4 group the Si—O bond length should be relatively small and it is expected to be increased by increasing charge and decreasing radius of the cation, which for hard metal cations are related to the EPA-properties.

Thus, the Pauling theory expresses the differences in covalency of Si—O bonds by varying the cationic species. In other words the intermolecular bond strength $\text{O} \rightarrow \text{M}$ should be related to the Lewis acid properties of the metal ion M and inversely related to the induced change in covalency of the adjacent intermolecular Si—O ($\rightarrow \text{M}$) bond.

In disilicates this effect induces further a decrease in Si—O—Si bridging distances as the result of secondary inductive effects.



If the metal ions are Si^{4+} , which act as strong Lewis acids, the SiO_2 structure is completed, where the Si—O distances of 1.60 Å are considerably shorter than in silicate chains, for example 1.65 Å in lithium disilicate [69].

There is a functional relationship between bond strength and bond length regardless of structure type [66] with the constraint that the sum of the bond strengths equals the valence as proposed by Pauling. Brown and Shannon [66] analyzed environments of 884 cations in 417 different structures and have shown the agreement between experimental data and the Pauling concept for the majority of atoms in the first half of the periodic table.

Noll [68] has demonstrated the usefulness of the application of the electronic theory to silicates and organopolysiloxanes. His starting point is the three dimensional network of SiO_2 . Substitution of Si^{4+} ions by cations of lower charge was found to be reflected in variations of bond lengths and physical properties explained in terms of variations of inductive effects due to the differences in coordinating interactions between the metal cations and the silicate anions. The Si—O distance is shortest in SiO_2 , namely 1.60 Å because —Si—O groups are coordinated by Si^{4+} ions. Substitution of the latter by ions

TABLE 9

Si—O distances in some silicate structures (Å) [68]

| Silicate | Formula | Si—O (\rightarrow Si) (mean value) | Si—O (\rightarrow M) (mean value) |
|---------------------|--|--|---|
| Sodium metasilicate | $\text{Na}_4[\text{Si}_2\text{O}_6]$ | 1.675 | 1.57 |
| Enstatite | $\text{Mg}_2[\text{Si}_2\text{O}_6]$ | 1.60 | 1.55 |
| Diopside | $\text{MgCa}[\text{Si}_2\text{O}_6]$ | 1.62 | 1.57 |
| Pigeonite | $(\text{Mg,Fe,Ca})_2[\text{Si}_2\text{O}_6]$ | 1.64 | 1.58 |
| Li-disilicate | $\text{Li}_2[\text{Si}_2\text{O}_5]$ | 1.65 | 1.56 |
| Na-disilicate | $\text{Na}_2[\text{Si}_2\text{O}_5]$ | 1.64 | 1.51 |
| Sanbornite | $\text{Ba}_4[\text{Si}_8\text{O}_{20}]$ | 1.66 | 1.60 |

of lower charge leads to a decrease in the coordinating interaction, since the EPA properties of the metal ions decreased by decrease in charge, e.g. the O—Si bond is stronger than the O—Al bond. With reference to the acidity of Si^{4+} , the substituted metal ions are considered as electron donors towards the O—Si bond and this provokes a decrease in Si—O bond distance. As a secondary effect, an increase in Si—O—Si bond distances is observed, both effects increasing with increasing electron donor properties, e.g., with decreasing EPA properties of the metal ions. The effects are in the opposite direction, when metal ions with increasing EPA properties (decreasing donor properties according to Noll) are considered (Table 9).

The effects are greater in polymeric structures of elements of higher charge, e.g. in phosphates or sulfates and this is actually found (Table 10).

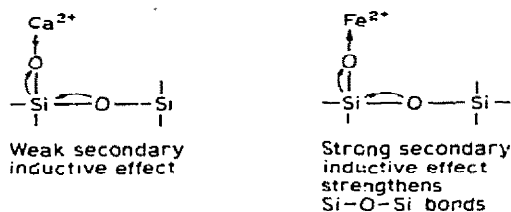
The differences in bond length are reflected in differences in chemical reactivities. Indeed, small differences in bond strength may provide remarkable differences in chemical behaviour. Weitz [70] has shown that acetic acid heterolyses the Si—O—Si bonds to a greater extent in Wollastonite than it does in Hypersthene. Both compounds are chain structures, but Wollastonite contains Ca^{2+} ions and Hypersthene Mg^{2+} and Fe^{2+} ions. The differences in EPA properties lead to differences in Si—O—Si bond strengths, which are weaker

TABLE 10

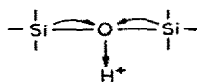
P—O, As—O, S—O (X—O) distances in phosphate, and sulfate lattices (Å) [68]

| Formula | X—O (\rightarrow X) (mean value) | X—O (\rightarrow M) (mean value) |
|--|--|--|
| RbPO_3 | 1.62 | 1.45 |
| LiAsO_3 | 1.77 | 1.60 |
| NaAsO_3 | 1.77 | 1.67 |
| $\text{Na}_4\text{P}_2\text{O}_7 \cdot 10\text{H}_2\text{O}$ | 1.63 | 1.47 |
| $\text{K}_2\text{S}_2\text{O}_7$ | 1.64 | 1.44 |

in Wollastonite than in Hypersthene.

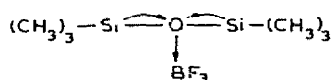


The great ease of acidolysis in the case of Wollastonite is due to the following facts: the greater electron density at the bridging oxygen atoms allows stronger electrophilic attack by the hydrogen ions, by which the polarity of the Si—O—Si is increased and eventually leads to heterolysis



For these reasons acidolysis leads to low molecular units with Wollastonite, and to polysilicates for Hypersthene.

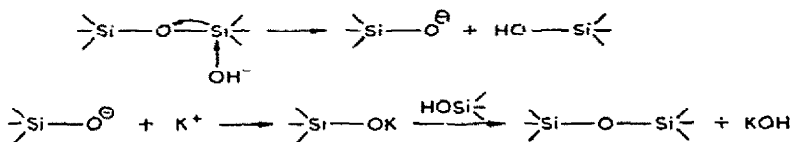
The bridging oxygen atom in silicates may be compared to that in siloxanes; hexamethyldisiloxane is attacked by the Lewis acid PF_3 , while hexachlorodisiloxane remains unaffected [68]: in the former the Si—O—Si bonds are more strongly polar and hence the bridging oxygen atom more basic than in the latter



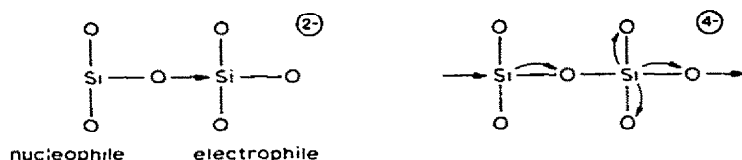
The replacement of Si^{4+} by $\text{Al}^{3+} + \text{K}^+$ reduces the extent of the inductive effects. This is in agreement with the old mineral chemical experience that Plagioclase shows increased instability towards acids with increasing Al content [68].

Noll [68] has also drawn attention to the electronic interpretation of the magmatic crystallization. The Si—O bond is most stable in SiO_2 and it is inductively labilized by substitution of Si^{4+} by cations of lower acidity. In the course of the crystallization of natural silicatic magmas the formation of crystalline phases follows the sequence of increasing inductive weakening of the Si—O—Si bonds by metal ions of decreasing Lewis acid properties.

In silica-rich melts polyanions are present in agreement with the mineralogical experience that silicate crystals with anions of high degree of coordination are more abundant than isolated groups. Noll [68] considers organopolysiloxanes as “weakened silicate melts”, which are subject to nucleophilic attack by hydroxyl ions.



Rearrangements are the result of alternating heterolysis and acid–base interactions which lead to equilibria between anions of different structures depending on the type and relative number of metal ions present. Particularly in metasilicate melts in the Si:O ratio 1:3, equilibria between ring and chain structures are readily established. At low temperatures the formation of chain like structures is preferred in agreement with Noll's second selection principle. Indeed, we shall see from the electronic consideration of association in liquid water that the acid–basic properties of the amphoteric water molecules are enhanced and in this way higher aggregates are readily formed. The acid–base interaction between 2 metasilicate anions leads to an increase in acidity at the silicon atom belonging to the nucleophilic anion, while the basicities of the terminal oxygen atoms are enhanced.



Chain propagation is sterically more likely than ring closure.

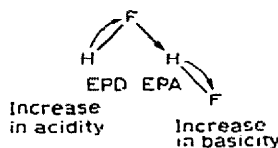
F. INDUCTIVE EFFECTS IN ASSOCIATION-PHENOMENA

Various hydrides, such as hydrogen fluoride, water, ammonia or the alcohols are associated in the liquid state through hydrogen bonding to different extents. It has recently been emphasized, that the electrostatic description of hydrogen bonding is rather unsatisfactory [5]. There is no relationship between the dipole moment of the base and the strength of the hydrogen bond, the atoms are found at much smaller distances than would be expected from the consideration of the van der Waals radii, and the IR intensities of the H–X stretch frequencies as well as the shifts observed in NMR data on hydrogen bridges cannot be explained by the electrostatic theory. It is, however, possible to treat the delocalization of the electrons in a semiquantitative way by means of LCAO–MO methods and numerous structural questions involved in hydrogen bonding are solved by these as well as by other semiempirical methods.

The dynamic features in the liquid state may be described in terms of proton transfer [71]. For the sake of including these interactions in the unified approach, the changes involved in electron distributions may be considered as being initiated by the exercise of the EPA function at the hydrogen atom and by the exercise of the EPD function at the functional group of the base. The final electronic arrangement is considered a result of the inductive effects caused by this primary interaction. In chains of HF molecules the energy of the hydrogen bond increases with increasing number n of HF-molecules in the chain: higher aggregates are energetically favoured [5].

Dimerization leads to an increase both in acidic character of the terminal hydrogen atom and in basic character of the terminal fluorine as a result of

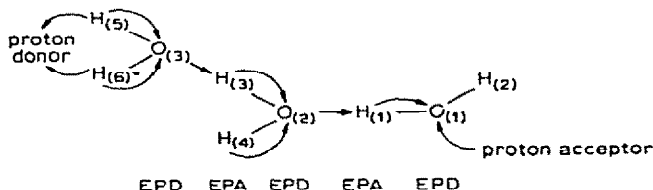
the charge-transfer occurring in the process of dimerization. In this way the formation of chains is favored.



The electronic rearrangement takes place throughout the chain in the same direction, and in this way the actual net charges at the atoms terminating the chain are increased. According to CNDO/2 calculations [5] the zig-zag structure of the HF chain offers an additional gain in energy. Such cooperative effects are also present in cyclic polymers which are also known to be present in the gas phase. The features are analogous to those in charge-transfer complexes.

Experimental evidence is available for water, the donicity for single water molecules being considerably lower than that of associated molecules, while the donicity of single water molecules is 18, the bulk donicity of liquid water is about 32 [35, 44, 72].

The association of water is presented in the following way [32].



Nucleophilic attack of a water molecule (oxygen atom $O_{(2)}$) at hydrogen atom $H_{(1)}$ of another water molecule induces polarization of the adjacent bonds and hence increasing acidities of the hydrogen atoms $H_{(3)}$ and $H_{(4)}$, as well as increasing the base strength of oxygen atom $O_{(1)}$. EPD—EPA interactions between the hydrogen atoms $H_{(3)}$, or $H_{(4)}$ (which are more acidic than $H_{(2)}$) and the oxygen atom $O_{(3)}$ of a water molecule will further increase both the acidity of the terminal hydrogen atoms $H_{(5)}$ and $H_{(6)}$ and the EPD strength of the terminal oxygen atom $O_{(1)}$. With increasing chain length this process may finally result in a proton transfer of an acidic hydrogen atom of one aggregate to the basic terminal oxygen atom of another aggregate and this process is known as autoprotolysis or self-ionization.

Recent quantum mechanical calculations strongly support this model. CNDO/2 calculations on linear chains of H_2O and HF molecules reveal (Table 11), that the mean energy ΔE of the hydrogen bonds is increasing with increasing chain length ("cooperative effect") [5]. Even more significant is the energy $\Delta E_{(n-1) \rightarrow n}$ for addition of the "last" solvent molecule, which is always higher than ΔE and clearly reflects the increasing acidity (basicity) of the terminal hydrogen and oxygen atoms, respectively (see Table 11).

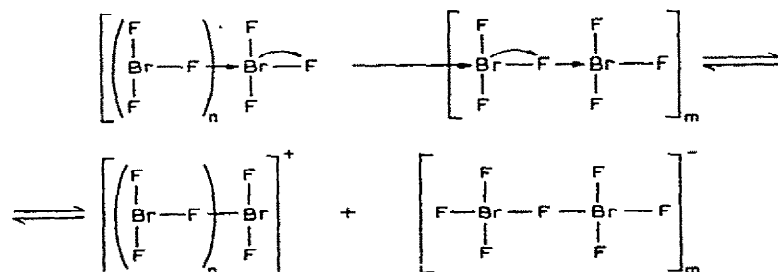
TABLE 11

Mean hydrogen bond energies for linear chains of H₂O and HF molecules as a function of chain length

| H ₂ O | | | HF | | |
|---------------------|-------------------|---|---------------------|-------------------|---|
| Number of molecules | ΔE (kcal) | $\Delta E_{(n-1) \rightarrow n}$ (kcal) | Number of molecules | ΔE (kcal) | $\Delta E_{(n-1) \rightarrow n}$ (kcal) |
| 2 | 8.68 | 8.68 | 2 | 9.50 | 9.50 |
| 3 | 9.63 | 10.59 | 3 | 10.88 | 12.25 |
| 4 | 10.12 | 11.11 | 4 | 11.62 | 13.12 |
| 5 | 10.43 | 11.34 | 5 | 12.08 | 13.45 |
| 6 | 10.61 | 11.44 | 6 | 12.38 | 13.60 |
| 7 | 10.78 | 11.50 | 7 | 12.60 | 13.68 |
| 8 | 10.98 | 11.54 | 8 | 12.76 | 13.72 |

Calculations for associated units with tetrahedral geometry which present a more realistic model for the structure of liquid water show similar trends although the effects are somewhat smaller [5]. It should perhaps be mentioned that elementary electrostatic models cannot account for the structure of hydrogen bonded associates: The electrostatic theory predicts a linear arrangement of H—F molecules as the most stable structure of the HF dimer, in contrast to quantum mechanical calculations [5] from which a bent structure is predicted in agreement with spectroscopic evidence.

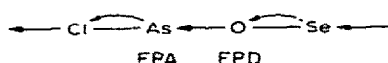
The existence of hydrogen bonds is not a necessary condition for association. The association in liquid hydrogen fluoride may be described either by hydrogen bridges between fluorine atoms or by fluorine bridges between hydrogen atoms [73]. In aprotic solvents, such as in bromine(III)fluoride, fluorine bridging is involved in associated solvent molecules. By the charge transfer taking place in the association process, the properties of the terminal atoms are changed: the fluorine atoms become more basic while the bromine atoms are increased in acidity as a consequence of the polarization of the bromine—fluorine bonds. These effects are expected to increase by increasing association, so that the interaction of highly associated units may produce ions (self-ionization).



Association and self-ionization may be described in an analogous manner for liquid iodine(I)-chloride, iodine(I)-bromide, antimony(III)-chloride, arsenic(III)-chloride or mercury(II)-bromide [35, 74].

It may be concluded that weak interactions between sufficiently amphoteric molecules may lead to strong interactions due to cooperative charge-transfer effects. This may be illustrated by the following example:

$(\text{SeO}_3)_4$ reacts with arsenic(III) chloride to give an insoluble polymer [75] while no reaction occurs with SO_2 , which is not sufficiently amphoteric. Raman spectrographic results indicate the presence of As—O—Se bonds. According to the functional presentation the formation of the coordinate bond between an oxygen atom of a selenium trioxide molecule and an arsenic atom induces a corresponding increase in EPA properties at the chlorine atoms bonded to arsenic and as well as an increase in EPA properties at the selenium atoms.



These changes favour the formation of coordinate bonds $\text{---Se} \leftarrow \text{Cl---}$, and these amplify the electron changes achieved so far, yielding a further increase in bond strength of both As—O and Se—Cl bonds. This type of interaction is not restricted to one dimension, as indicated in the formulation. The bonds between AsCl_3 and SeO_3 would be weaker, if the amphoteric properties of the molecules were developed to a lesser extent.

G. CONCLUSIONS

It has been shown elsewhere, that the functional approach is useful in gaining a unified description for the influence of solvents and of ligands on redox properties [44], the kinetics of substitution and redox reactions [7] as well as solvation phenomena [72] and the thermodynamics of ionic equilibria in different solvents [32, 35]. The extension of this approach to molecular interactions based on Lindqvist's theory for donor—acceptor interactions [1] allows a unified understanding of various phenomena, which are usually treated by entirely different approaches. Strong adducts, charge-transfer complexes, chemisorption, physisorption, association phenomena in the liquid phase as well as phenomena in the crystalline state have been shown to have much in common, in that in the course of the intermolecular interactions the adjacent intramolecular bonds are weakened and further electronic changes induced. Molecular properties, such as ionization potential of the donor and charge transfer energy of the complex cannot be regarded as a measure of the relative complex stability when different groups of compounds are considered. Functional parameters, such as donicity or basicity constants take their place.

It appears that "well-balanced" interactions are required to give a stable adduct, e.g. the energy provided by formation of the coordinate bond should not be considerably greater than the energy required to heterolyse the weakest

bond in the system. Since the Sb—Cl bonds are rather strong, strong adducts can be formed between SbCl_5 and strong Lewis bases. The weaker iodine—iodine bond is heterolyzed by excess pyridine and un-ionized molecular adducts are formed only when weak donors are provided. It is likely that analogous considerations may hold for very weak interactions, such as adhesion and other phenomena at interfaces.

More systematic research is required in order to establish these relationships more quantitatively and for a greater number of different types of adducts as well as to relate empirical parameters to complex stability and to changes in bond properties effected by adduct formation. It should then be possible to develop more precise theoretical interpretations and to allow semiquantitative predictions.

H. ACKNOWLEDGEMENTS

Thanks are due to the Fonds zur Förderung der wissenschaftlichen Forschung in Österreich for the continuous support of research on coordination phenomena. I also wish to express sincere thanks to all who gave their advice, namely Prof. H. Noller, Prof. P. Schuster, Dr. H. Voellenkle and Dr. H. Mayer.

I. REFERENCES

1. I. Lindqvist, *Inorganic Adduct Molecules of Oxo-Compounds*, Springer—Verlag, Berlin, Göttingen, Heidelberg 1963.
2. G. Briegleb, *Elektronen-Donator—Acceptor-Komplexe*, Springer—Verlag, Berlin, Göttingen, Heidelberg, 1961.
3. R. Foster, (Ed.), *Molecular Complexes Vol. 1*, Elek. Science, London, 1963.
4. R.S. Mulliken, W.B. Person, *Annu. Rev. Phys. Chem.*, 13 (1962) 107.
5. P. Schuster, *Z. Chem.*, 13 (1973) 41.
6. J. Rose, *Molecular Complexes*, Pergamon, London, 1967.
7. V. Gutmann and R. Schmid, *Coord. Chem. Rev.*, 12 (1974) 263.
8. H.A.O. Hill, J.M. Pratt and R.J.P. Williams, *Discuss. Faraday Soc.*, 47 (1969) 165.
9. R.S. Mulliken, *J. Amer. Chem. Soc.*, 72 (1950) 600; *J. Chem. Phys.*, 19 (1951) 514.
10. R.S. Mulliken, *J. Amer. Chem. Soc.*, 74 (1952) 811; *J. Phys. Chem.*, 56 (1952) 801.
11. R.S. Mulliken and W.B. Person, *Annu. Rev. Phys. Chem.*, 13 (1962) 107.
12. V. Gutmann and U. Mayer, *Rev. Chim. Miner.*, 8 (1971) 429.
13. C.K. Prout and J.D. Wright, *Angew. Chem.*, 80 (1968) 688.
14. *Chem. Soc. Publ. Nr. 11 (1958) Tables of Interatomic Distances and Configuration in Molecules and Ions.*
15. J.L. Hoard, S. Geller and T.B. Brown, *Acta Crystallogr.*, 4 (1951) 405.
16. V. Gutmann and K.H. Wegleitner, *Z. Phys. Chem. (n.F.)*, 17 (1972) 77.
17. H. Kietzbl, H. Völlenkle and A. Wittmann, *Monatsh. Chem.*, 103 (1972) 1360.
18. Y. Hermodsson, *Ark. Kemi*, 31 (1969) 218.
19. W.H. Zachariasen, *J. Chem. Phys.*, 1 (1933) 634; R.L. Sass and R.F. Scheuermann, *Acta Crystallogr.*, 15 (1962) 77.
20. O. Hassel and C. Rømming, *Quart. Revs.*, 16 (1962) 1.
21. R.S. Mulliken and W.B. Person, *Molecular Complexes*, Wiley-Interscience, London, New York, 1969.

22. K.O. Strømme, *Acta Chem. Scand.*, 13 (1959) 268.
23. O. Hassel and N. Hoppe, *Acta Chem. Scand.*, 14 (1960) 341.
24. E.M. Kosower, S.G. Cohen, A. Streitwieser Jr. and R.W. Taft, *Progr. Phys. Org. Chem.*; Ed. 3, (1965) 80.
25. O. Hassel and J. Hroslev, *Acta Chem. Scand.*, 8 (1954) 873.
26. O. Hassel and K.O. Strømme, *Acta Chem. Scand.*, 13 (1959) 1775.
27. O. Hassel and K.O. Strømme, *Acta Chem. Scand.*, 12 (1958) 1146.
28. K. Niendorf and R. Paetzold, *J. Mol. Struct.*, 19 (1973) 693.
29. K. Burger and E. Fluck, *Inorg. Nucl. Chem. Letters*, 10 (1974) 171.
30. P.M. Spaziant and V. Gutmann, *Inorg. Chim. Acta*, 5 (1971) 273.
31. H.S. Gutowsky and C.J. Hoffmann, *J. Chem. Phys.*, 19 (1951) 1259.
32. U. Mayer and V. Gutmann, *Advances Inorg. Nucl. Chem.* (Ed. H.J. Emeléus, A.G. Sharpe) Vol. 17, in the press.
33. M. Herlem and A.I. Popov, *J. Amer. Chem. Soc.*, 94 (1972) 1431.
34. M. Yamada, H. Saruyama and K. Aida, *Spectrochim. Acta*, 28A (1972) 439.
35. V. Gutmann, *Angew. Chem.*, 82 (1970) 858, int. Ed., 9 (1970) 843; *Chem. Brit.*, 7 (1971) 102; *Topics in Current Chem.*, 27 (1972) 59.
36. A.F. Wells, "Structural Inorganic Chemistry", 3rd Ed. Clarendon Press, Oxford, 1962.
37. H. Zeiss, "Organometallic Chemistry", ACS-Monograph Series, p. 477, Reinhold, 1960.
38. B. Beagley, D.W.J. Cruickshank, P.M. Pinder, A.G. Robiette and G.M. Sheldrick, *Acta Crystallogr.*, B 25 (1969) 737.
39. P.A. Agron, R.D. Ellison and H.A. Levy, *Acta Crystallogr.*, 23 (1967) 1079.
40. G.S.D. King, *Acta Crystallogr.*, 15 (1963) 243.
41. J. Degréve, J. Meunier-Piret, M. Van Meerssche and P. Piret, *Acta Crystallogr.*, 23 (1967) 119.
42. L. Rodrique, M. Van Meerssche and P. Piret, *Acta Crystallogr.*, B 25 (1969) 519.
43. P. Piret, J. Meunier-Piret and M. Van Meerssche, *Acta Crstallogr.*, 19 (1965) 78.
44. V. Gutmann, *Struct. and Bonding*, 15 (1973) 141.
45. A.F. Cotton and G. Wilkinson, "Advanced Inorganic Chemistry" Interscience, 1967.
46. W. Beck and K. Lottes, *Z. Naturforsch.*, 19b (1964) 987.
47. G.G. Sumner, H.P. Klug and L.E. Alexander, *Acta Crystallogr.*, 17 (1964) 732.
48. M.L. Hair, *Infrared Spectroscopy in Surface Chemistry*, Dekker, New York, 1967.
49. L.H. Little, *Infrared Spectra of Adsorbed Species*, Academic Press, London, New York, 1966.
50. J.T. Yates Jr., C. and EN, Aug. 26, 19 (1974).
51. H.P. Leftin and M.C. Hobson Jr., *Advan. Catal. Relat. Subj.*, 14 (1963) 150.
52. H.A. Benesi and A.C. Jones, *J. Phys. Chem.*, 63 (1959) 179.
53. G.A. Galkin, A.V. Kiselev and V.I. Lygin, *Russ. J. Phys. Chem.*, Engl. Transl., 36 (1962) 951.
54. H. Noller and P. Horill, Private Communication.
55. D.J.C. Yates and P.J. Lucchesi, *J. Chem. Phys.*, 35 (1961) 243.
56. G. Kortüm, J. Vogel and W. Braun, *Angew. Chem.*, 70 (1958) 651.
57. J.T. Yates Jr. and D.A. King, *Surface Sci.*, 30 (1972) 601.
58. J.T. Yates Jr., T.E. Madey and N.S. Erickson, *Surface Sci.*, 43 (1974) 257.
59. T. Ukaji and K. Kuchitsa, *Bull. Chem. Soc. Japan*, 39 (1966) 2153.
60. F. van Bolhuis, P.B. Koster and T. Mighelsen, *Acta Crystallogr.*, 23 (1967) 90.
61. C.H. Townes and B.P. Dailey, *J. Chem. Phys.*, 20 (1952) 35.
62. T. Mighelsen and A. Vos, *Acta Crystallogr.*, 23 (1967) 796.
63. C. Knobler, C. Baker, H. Hope and J.D.M. McCullough, *Inorg. Chem.*, 10 (1971) 697.
64. J. Berkowitz and W.A. Chupka, *J. Chem. Phys.*, 29 (1958) 653, 1386.
65. L. Pauling, *J. Amer. Chem. Soc.*, 51 (1929) 1010.
66. I.D. Brown and R.D. Shannon, *Acta Crystallogr.*, A 29 (1973) 266.
67. W.H. Baur, *Amer. Mineral.*, 56 (1971) 1573.
68. W. Noll, *Angew. Chem.*, 75 (1963) 123.

69. F. Liebau, *Acta Crystallogr.*, 14 (1961) 389.
70. E. Weitz, H. Franck and M. Schuchard, *Chem. Ztg.*, 74 (1950) 256.
71. F.B. van Duijnerveldt, *J. Chem. Phys.*, 49 (1968) 1424.
72. U. Mayer and V. Gutmann, *Struct. and Bonding*, 12 (1972) 113.
73. V. Gutmann, *Sv. Kem. Tidskr.*, 68 (1956) 1.
74. V. Gutmann, "Coordination Chemistry in Non Aqueous Solutions" Springer—Verlag, Vienna, New York, 1968.
75. K. Dostal and J. Toucin, Private Communication.